RSC Advances

This article can be cited before page numbers have been issued, to do this please use: U. Shanker, V. Jassal and M. Rani, *RSC Adv.*, 2016, DOI: 10.1039/C6RA17555D.

ROYAL SOCIETY OF CHEMISTRY

www.rsc.org/advances

View Article Online
DOI: 10.1039/C6RA17555D

Catalytic removal of organic colorants from water using some transition metal oxide nanoparticles synthesized under sunlight

Uma Shanker,* VidhishaJassal and Manviri Rani

*Department of Chemistry
Dr B R Ambedkar National Institute of Technology
Jalandhar, Punjab, India-144011

* Corresponding Author
Dr Uma Shanker
(Assistant Professor)
Office Number-CE-306
Department of Chemistry
Dr B R Ambedkar National Institute of Technology Jalandhar,
Jalandhar, Punjab, India-144011
Email: shankeru@nitj.ac.in, umaorganic29@gmail.com
Contact number: +91- 7837-588-168 (Mobile)
+91-0181-269-301-2258 (Office)
Fax: +91-0181-269-0932

View Article Online
DOI: 10.1039/C6RA17555D

Abstract

Transition metal oxides (TMO) constitute most amazing class of materials with wide range of properties and applications. Therefore, their synthesis usinggreen approach is the need of present time. Hence, based on it, sunlight irradiation was employed to synthesize variousTMOnanostructures (ZnO, CuO, Co_3O_4,NiO and Cr_2O_3) using water as a solvent.Nanoparticles obtained with distinct morphologiessuch asnanotubes (ZnO; <35 nm), nanorods (CuO; 7-50 nm), nanorods, triangles and hexagons (Co_3O_4; 45-90 nm), needle-shaped (NiO; 2-25 nm) and nanobeads (Cr_2O_3;~17 nm) were confirmed by TEM analysis.The significance of synthesis is in its quick approach with no thermal heat involvement, reusable catalyst, cost effectiveness and ability to fabricate almost uniformly distributed nanoparticles with small sizes.The potential of nanoparticles synthesized was examined in treatment of simulated water containing hazardous dyes: Alizarin Red S (ARS) + Methylene Blue (MB). Interestingly, in a short period of 180 min 88.24% of the dyes mixture was more or less completelydegraded using Cr_2O_3nano-needles followed by 87.96% (ZnO) > 86.86% (CuO) > 85.89% (NiO) > 80.35% (Co_3O_4), depending on the sizes of respective TMO nanoparticles. This is also supported by finding of small and non-toxic by-productssuch as but-2-enal, sulfur trioxide and benzoquinone. With high potential observedin removal of dyes, TMO nanoparticles can be used as important adsorbents in waste water treatment with a bright future. The advantage of present work lies in its green synthesis of nanoparticles and their application in making our environment green.

Keywords: green synthesis, sunlight, TMO nanoparticles, morphology, dyes removal.

View Article Online
DOI: 10.1039/C6RA17555D

1. Introduction

Transition metal oxides (TMOs) are an important class of materials due to their several attractive properties such as magnetic, electronic and optical.[1,2] This makes them effective to be used in the variety of applications such as catalysis,[3] sensors,[4] lithium ion batteries[4,5] and many more.[6,7] Concerning to these applications, TMOs are advantageous as compared to the other conventionally used materials. Therefore, their synthesis using advanced methods is the key interest of researchers around the globe.

In general, various methods based on the dry and wet procedures have been developed for the synthesis of TMO nanoparticles.[8,9] However, such methods have disadvantages in terms of temperature and requirement of toxic chemical reagents that may harm the environment. To overcome the negative effects of these problems, the best possible way is to move towards green chemistry, i.e. avoiding the use of hazardous reagents and replacing them with the natural ones in all the technological processes.[10] Along with the reduction in environmental pollution,[11] green routes yield contaminants free nanoparticles with small size and distinct morphology.[12,13] Following the green chemistry principles, authors decided to employ a sunlight assisted approach for the synthesis of various TMO nanoparticles, namely, zinc oxide (ZnO), chromium oxide (Cr_2O_3), cobalt oxide (Co_3O_4), copper oxide (CuO) and nickel oxide (NiO) nanoparticles.

Recently, the applications of TMO nanoparticles in the treatment of wastewater containing organic colorants have gained immense interest owing to their high surface area and semiconducting properties.[14] Irregular and unsystematic use of dyestuffs is a glaring evidence of environmental pollution. Textile and paper industries discharge the enormous volume of pollutants, non-degradable and carcinogenic natured colored dye effluents into the water bodies without any proper treatment, thus leading to the contamination of water resources.[15] Therefore,

View Article Online
DOI: 10.1039/C6RA17555D

it is a matter of utmost importance to eliminate the dyestuffs from water bodies. Recently, authors reported the degradation of malachite green and eriochrome black T using potassium zinc hexacyanoferrate nanoparticles.[16] This motivated us to explore the effective use of other nanoparticles such as TMO in the degradation/removal of hazardous organic dyes.

The dye Alizarin red S (ARS) has been considerably used in the textile industry since ancient times.[17]ARS (1,2-dihydroxy-9, 10-anthra-quinonesulfonic acid sodium salt) is a water- soluble, widely used anthraquinone dye with carcinogenic effects and its release in environment can cause serious problems to human beings and animals. ARS is resistant to degradation because of its complex aromatic structure, high thermal and optical stability. Therefore, an effective catalyst is required for the degradation of ARS.[18] Methylene blue (MB) is widely used in coating for paper stocks, coloring paper, dyeing cottons, wools, *etc*. Acute exposure of MB will result in increased heart rate, vomiting, shock, Heinz body formation, cyanosis, jaundice and quadriplegia and tissue necrosis in humans.[19,20] Due to their wide use, toxicity, high persistence and bioaccumulation, authors selected these dyes for observing the potential of synthesized TMO nanoparticles in removal from simulated water.

In the light of above facts, it was planned to carry out green synthesis of various TMO nanoparticles using sunlight irradiation technique. In this method reaction was carried out by exposing the metal salt solution in sun light for one hour followed by addition of aqueous NaOH solution. Immediate precipitation of metal oxide nanoparticles occurred. Further characterization reveals the well-defined morphologies and uniform distribution of nanoparticles. The green synthesized TMO nanoparticles were employed for the treatment of simulated water containing ARS+MB dye mixture, which constitutes the hazardous discharge from industries into the water bodies. Various process parameters such as concentration of mixed dye solution, dose amount of catalysts used and pH of mixed dye solution were optimized. To the best of our knowledge, so

View Article Online
DOI: 10.1039/C6RA17555D

far no such method has been reported for the sunlight assisted green synthesis of TMO nanoparticles and their use in removal of these dyes from simulated water.

2. Experimental

Zinc nitrate ($Zn(NO_3)_2$), copper nitrate ($Cu(NO_3)_2$), cobalt nitrate ($Co(NO_3)_2$), nickel nitrate ($Ni(NO_3)_2$), chromium nitrate ($Cr(NO_3)_3$) and sodium hydroxide (NaOH) used in this study were of analytical grade and procured from Merck. All solutions were prepared using double distilled water.

2.1 Design of Experiment

2.1.1 Green synthesis of TMO nanoparticles

The aqueous solutions (0.05M, 100 ml) of different metal salts were prepared using double distilled water. The solution as such was kept in sunlight for 1 hour followed by addition of aqueous NaOH solution. Immediate precipitation of metal oxide nanoparticles occurred, which were then filtered, washed and dried in oven for further characterization.

Reactions were investigated under both with and without photo-illumination. No precipitation was observed without photo-illumination, whereas immediate precipitation of the TMO nanoparticles was observed within 1 hour under photo-illumination. The reason might be the presence of greater number of photons of certain wavelength in direct sunlight which initiate the reaction, thus promoting the formation of TMO nanoparticles.[21-23]

Initially the metal nitrate reacts with the sodium hydroxide to form $[M(OH)_x]^+$, as shown below:

$$M(NO_3)_x + NaOH \longrightarrow [M(OH)_x]^+$$

When the aqueous mixture was kept under sunlight irradiation, following process occurs:

$$H_2O \longrightarrow e^- + H_3O^+ + H_2 + \dot{H} + \dot{O}H + H_2O_2$$

View Article Online
DOI: 10.1039/C6RA17555D

The solvated electrons and free radicals are highly active species which helps in generating TMO nanoparticles.

$$[M(OH)_x]^+ + e^- + \dot{O}H \longrightarrow M_xO_y + H_2O$$

2.1.2 Photocatalyticdegradation studies in simulated water

The mixture of two dyes, namely, ARS (λ_{max} = 510 nm) and MB (λ_{max} = 665 nm),were used as a model system for photocatalytic dye removal experiments. Practicality of this particular application lies in the fact that industrial effluents contain a mixture of colored dyes which are being discharged untreated into the water reservoirs. A 50-ml of dye solution at various concentrations (10-50 mg/L) was prepared and metal oxide (5-25 mg) nanoparticles were added to it. The solutions were kept under bright sunlight. At different time intervals (20 minutes), 2-ml of the aliquots was taken and centrifuged at 10,000 rpm for 10 min. The absorbance spectrum of the supernatant was subsequently measured and continued upto 180 minutes.

Different parameters (Figure 5) such as catalyst amount, initial concentration and initial pH of mixed dye solution were optimized in order to get maximum dye degradation (%) by synthesized TMO nanoparticles. These collected samples were also analyzed for the identification of possible degradation products.

2.2 Instrumentation

Powder X-ray diffraction (PXRD) was recorded on a PAN analytical X-PRT PRO instrument using CuKα (λ=1.5406 Å) radiation. Field-Emission Scanning Electron Microscopy (FE-SEM) was performed in order to find out the surface morphology and average particle size of the synthesized TMO nanoparticles (Quanta 200 FEG). Exact particle size and shape of the nanoparticles was studied using Transmission Electron Microscopy (TEM) conducted with Hitachi (H-7500) instrument operating at 120kV. Malvern Zetasizer (Nano ZS) instrument was

View Article Online
DOI: 10.1039/C6RA17555D

used to measure the zeta potential of nanoparticles.

A spectrophotometer (Agilent Pro) was used for quantitative measurement of dyes. A gas chromatograph GC 1300 coupled with mass spectrometer TSQ8000 was used for identification of oxidative degradation products. Column used was TG 5MS having dimensions 30m × 0.2mm × 0 × 2mm. The conditions for GC were: injector temperature, 280 ºC and transfer line temperature, 250 ºC. The capillary column temperature was programmed 80 ºC for 2 min; from 80 to 260 ºC at 10 ºC min^{-1} and holding at 250 ºC for 15 min. Helium was used as a carrier gas with a flow rate of 2 ml min^{-1}. The mass spectrometer conditions were ion source at 250 ºC and ionization energy 40 eV.

3. Results and Discussion

Employing a green pathway based on sunlight and water, various TMO nanoparticles were synthesized successfully. Their detailed structural morphology and potential for degradation of hazardous dyes mixture are discussed. The PXRD, FE-SEM/EDS and TEM images are shown by Figures 1, 2 and 3, respectively.

3.1 Powder X-Ray Diffraction

PXRD data was found to be concordant with the JCPDS data (ZnO Card No.79-2205, CuO Card No. 80-1917, Co_3O_4 Card No. 76-1802, NiO Card No. 22-1189, Cr_2O_3 Card No.-76-0147). The peaks of the XRD spectra confirm the formation of respective products (Figure 1). The symmetry of the as synthesized TMO nanoparticles obtained was: Hexagonal (ZnO), Monoclinic (CuO), Cubic (Co_3O_4), Rhomohedral (NiO) and Rhombohedral (Cr_2O_3). Absence of secondary peaks ensures high purity level of the samples. In case of ZnO, CuO, Co_3O_4, NiO and Cr_2O_3 the maximum relative intensity (%) was observed at 17.47º, 25.26º, 25.04º, 25.02º and 33.67º at 2θ scale, respectively (Table 1-S). A comparison was also carried out with traditionally used

View Article Online
DOI: 10.1039/C6RA17555D

methods to confirm the effectiveness of the current approach. Nugroho and Kim 2014 synthesized Co_3O_4 nanoparticles with high crystalline size and low crystallanity at low concentrations of KOH using supercritical water.[24] A thermal treatment method was also employed to synthesize crystalline Co_3O_4 nanoparticles with no peaks of impurities.[25] Various other methods are also reported for the synthesis of cobalt oxide nanoparticles such as mechanochemical, micro-emulsion, *etc*.[26, 27] Employing a sol-gel technique NiO nanoparticles having average size of 5 nm and rock-salt structurewere synthesized.[28] Heat-treated and cubic nickel oxide nanoparticles with high level of purity have also been synthesized.[29, 30] Gibot and Vidal synthesized well-crystalline Cr_2O_3 nanoparticles (with no impurities of silica)using Cr (III) nitrate and nanometric silica spheres as precursor and template agent, respectively.[31] Magnetic chromium oxide nanoparticles were also synthesized via simple approach.[32] Through electrochemical method ZnO nanoparticles with high crystallanity were synthesized.[33] Various other techniques like micro-emulsion, thermal treatment, *etc* also resulted in monodisperse ZnO nanoparticles.[34-36] Good crystallanity of CuO nanoparticles was obtained using $Cu(NO_3)_2$ as precursor as compared to $CuCl_2$ precursor, with increase in crystallanity after annealing.[37] A thermal decomposition route was employed for synthesizing copper oxide nanoparticles with high purity level.[38] Using carbon nanotubes as template, Wu *et al*. (2002) synthesized CuO nanoparticles with average size ~ 37.2 nm, as confirmed by XRD analysis.[39] Though our results are similar to these conventional methods such as electrochemical or sol-gel providing the nanosize crystaline TMOs but green approach is best among because of easy to perform and a good alternative to the earlier time consuming and costly methods.

View Article Online
DOI: 10.1039/C6RA17555D

3.2 FE-SEM

It is interesting to note here that even though all the TMOs were synthesized via same method but they exhibited different morphologies and were distributed almost uniformly throughout the network(Figure 2). Long uniform channels of ZnO nanoparticles(<50 nm) were formedin shape of tubes. Long rods nanoparticles of CuOhaving average size less than 100 nm were observed. Almost hexagonal shaped Co_3O_4 nanoparticles (50-100 nm) were formed. The average particle size in case of NiO and Cr_2O_3 nanoparticles was extremely small (<10 nm).

The EDS (Energy Dispersive X-Ray Spectroscopy) analysis of all the samples indicated the presence of oxygen along with concerned metal ion (Figure 2). In ZnO, Zn and O showed 80.07 and 19.93 weight (%) and 49.58 and 50.42 atomic (%), respectively. In case of CuO, weight (%) of Cu and O were 72.99 and 27.01, respectively, whereas atomic (%) were found to be 40.49 and 59.51, respectively. In Co_3O_4, Co and O exhibited 69.57 and 30.43 weight (%), on the other hand atomic (%) was found to be 38.29 and 61.71, respectively. Also, in case of NiO, weight (%) of Ni and O correspond to 66.52 and 33.48 and atomic (%) was 35.13 and 64.87, respectively. In Cr_2O_3, Cr and O exhibited 49.95 and 50.05 weight (%) and 23.49 and 76.51 atomic (%), respectively.

3.3 TEM

Small nanotubes of ZnO having size less than 35 nm were formed. Attractive morphology of CuO i.e. long nanorods (diameter7-50 nm) was observed. It is important to note that in case of Co_3O_4, three types of nanostructures namely, nanorods, triangular and hexagonal shapedwere observed. The length of the nanorods varied between 50-100 nm whereas diameter was less than 50 nm. The particle size of triangular and hexagonal shaped Co_3O_4 nanoparticles were also less than 50 nm. Needle-shaped NiO nanoparticles having extremely small size (length and width less

View Article Online
DOI: 10.1039/C6RA17555D

than 25 and 2 nm, respectively) were formed. Moreover, nanobeads of Cr_2O_3were formed with size ~17 nm. The most interesting feature of this study is the formation of various TMO nanoparticles with unique morphologies and sizes less than 100 nm (Figure 3).

3.4Application of TMO nanostructures in removal of hazardous dyes

The photocatalytic activity of the above synthesized TMO nanoparticles was evaluated for the removal of mixture of two dyes, namely, ARS and MB. Concentration was found to decrease continuously with increase in time interval. Under optimized conditions, the photocatalytic removal capacity of various nanostructures was observed to be: Cr_2O_3 (88.24%) >ZnO (87.96%) >CuO (86.86%) >NiO (85.89%) > Co_3O_4 (80.35%), depending on the size of nanoparticles formed.

Previous studies reported by researchers shows that maximum dye (Congo Red) degradation of 81.33% was achieved using ZnO nanoparticles synthesized via sol-gel method.[40] Also, degradation efficiency of ~72% was achieved using ZnO as a photocatalyst.[41] 87% of methyl violet was degraded using ZnO nanoparticles using precipitation technique.[42] Degradation of ARS under UV light irradiation was carried out using ZnO nanoparticles (~77% degradation in 90 minutes).[43] Moreover, CuO nanostructures synthesized via hydrothermal route were able to degrade methylene bue only in the presence of H_2O_2 as an oxidizing agent.[44] This proves the effectiveness of the above synthesized nanoparticles which can degrade dyes in the absence of any external oxidizing agent. Vaseem *et al*. (2008) utilized CuO nanoparticles for degrading MB dye. Results revealed the lower catalytic efficiency of the catalyst as negligible amount of dye got degraded.[45] Thus, it is clear from the above discussion that TMO nanoparticles synthesized via sunlight mediated green route have better catalytic efficiency for the removal of organic dyes

View Article Online
DOI: 10.1039/C6RA17555D

than the conventional TMO nanoparticles. Also, these nanomaterials are cost-effective, hence, can be employed on a larger scale for degrading hazardous organic dyes

3.4.1 Effect of dye concentration

To estimate the initial concentration of dyes which can be effectively degraded using synthesized nanoparticles, experiments were carried out for various concentrations of the dye solution (10-50 mg/L; catalyst loading-15mg/10 ml; pH=7.0). Maximum removal of dyewas obtained at 10 mg/L (Figure 5a), which is probably due to the fact that at low dye concentration more number of active sites are available for adsorption by catalyst. As the concentration increases, the surface area of the catalyst becomes limited, i.e. catalyst:reactant ratio decreases. Hence, responsible for the decreased rate of dye removal.[46]

3.4.2 Effect of pH

pH of solution is the most important parameter for measuring the photocatalytic efficiency of nanoparticles. It was observed that the dye removal increased with the raising pH upto 7.0, after that it got decreased (dye concentration-10mg/L; catalyst loading-15mg/10 ml) (Figure 5b). This may be due to the ion screening effects of H^+ ions under acidic conditions and OH^- ions in alkaline medium which mayhave the adverse impact on the adsorption and hence less dye decoloration was observed.[47] In acidic medium H^+ ions may get attracted towards the dye molecules and in alkaline medium OH^- ions may get adsorbed on the surface of photocatalyst. Thus, decreasing the rate of photodegradation. Therefore, at neutral pH interference from other ions is not observed and best results were obtained. Moreover, according to the point of zero charge (Pzc), the surface charge properties of TMOs changes with change in pH of the solution. The Pzc for TMO is around 6.5-8.0, thus, the surface is presumably positively charged in acidic

View Article Online
DOI: 10.1039/C6RA17555D

medium (pH<Pzc) and negatively charged in basic medium (pH>Pzc).[48, 49] MB is cationic dye whereas ARS is anionic, thus mixing the two dyes of equal concentrations is believed to give a neutral solution. For better understanding of effect of pH, Zeta potential, of the TMOs at neutral pH was recorded and as per established fact that surface charge can greatly influence the stability of nanoparticles through the electrostatic repulsion between the particles. Greater the zeta potential, more is the probability of particles to be stable because the charged particles repel one another and hence overcome the usual tendency to aggregate.[50] The negative zeta potential values of ZnO, CuO, Co_3O_4, NiO and Cr_2O_3, i.e. -16.5, -11.5, 3.07, -11.6 and -25.2 mV, respectively were observed at neutral pH (Figure 4). The high absolute zeta potential value specifies a strong repellent force among the nanoparticles which ultimately prevents aggregation .[51, 52] Among the nanoparticles used, Cr_2O_3 is having the highest absolute value of zeta potential, thus, justifying its greater surface activity.

3.4.3 Effect of catalyst loading

The rate of removal of hazardous dyes as a function of initial amount of photocatalyst (5mg/10 ml to 25 mg/10 ml) has been examined. The results(Figure 5c) show that removal of dye continuously increased with increasing dosage of the catalysts, reached the higher value (at 15mg/10 ml) and then decreased. The probable reason could be that as the dose increases, the number of active sites on catalystpenetratedbyphotons gets blocked, thereby, decrease in the rate of removal of dyes were observed.[53]

3.5 Reaction mechanism

TMOs (ZnO, CuO, Co_3O_4, NiO and Cr_2O_3) being semiconducting in nature are able to generate electron-hole pair (in conduction and valence band, respectively) upon photoillumination. The interaction of these electron-hole pairs with water produces active species $OH^{\bullet}$ which breaks the

View Article Online
DOI: 10.1039/C6RA17555D

large harmful organic dyes (Figure 6). First, adsorption of the dye takes place on the surface of adsorbent (TMO nanoparticles), followed by dye degradation process.[54] Overall, the generation of electron-hole pairs cum $OH^{\bullet}$ is responsible for the photodegradation of different organic dyes as well as other organic pollutants. Electrons in the conduction band on the surface of catalyst can reduce to molecular oxygen into superoxide ion, which ultimately forms hydrogen peroxide. The holes generated in situ are responsible for the generation of hydroxyl radicals which are the primary agents responsible for the cleavage of dye minerlization.[47]

3.5.1 Adsorption isotherms

Adsorption isotherms (Figure 7a) of ARS+MB clearly show that adsorption is fast in all the cases and the isotherms are regular, positive and concave to the concentration axis. Adsorption data can be represented through Langmuir adsorption isotherms which assume the formation of a monolayer of solute molecules on the surface of the adsorbent.[55] A typical graph of C_e/X_e v/s C_e of all the dyesis a straight line (Figure 7b). The adsorption data was fitted in Langmuir adsorption equation:

$$\frac{C_e}{X_e} = \frac{1}{k_L X_m} + \frac{C_e}{X_m}$$

or

$$\frac{1}{X_e} = \frac{1}{C_e}\left(\frac{1}{k_L X_m}\right) + \frac{1}{X_m}$$

Where, C_e is the equilibrium concentration of the dye solution; X_e the amount of dye adsorbed per gram weight of adsorbent; X_m the amount of dye adsorbed at saturation; k_L the Langmuir adsorption constant. X_m, k_L and R^2 values were determined to be: ZnO (18.587; 4.744; 0.985), CuO (19.696; 4.896; 0.933), Cr_2O_3 (18.663; 4.969; 0.988), Co_3O_4 (22.183; 13.254; 0.777) and NiO (22.306; 7.686; 0.905).

View Article Online
DOI: 10.1039/C6RA17555D

3.5.2Photocatalytic degradation products of ARS and MB using TMO Nanoparticles

It has been found that under neutral conditions (pH~7.0) solid-support oxidative process resulted in the formation of colorless products which got deposited over the surface of TMO nanoparticles. Possible degradation pathway of oxidative degradation of ARS and MB and their representative mass spectrum are shown in Figures 8 and 9, respectively.

3.5.3 Identification of products by GC-MS analysis:

An attempt has been made to propose the degradation pathway of the major products formed via hydrolysis or oxidation of the dyes mixture. The identification of the products has been done using earlier reported literature as well as NIST library inbuilt with GC-MS system. The major oxidative agent is $OH^{\bullet}$ which is highly active species and is known to degrade the complex dyes into smaller by-products.[47] Complete mechanism leading to the generation of $OH^{\bullet}$ is represented in Figure 10. ARS (mol.wt. = 342) present in the dye mixture undergoes attack by O_2 radical at C-12 position under visible irradiation (1; sodium-3,4-dihydroxy-9,10-dioxo-9,10-dihydroanthracene-2-sulfonate). This causes the dye to cleave into two parts: one part gets oxidized to phthalic acid (1a; molecular ion peak at m/z=166) and the other part is oxidized to hydroxyl intermediates (1b) which finally gets mineralized into CO_2 and SO_4^{2-} ions.[56] After the hydrolysis of MB (mol.wt.=320), (2; 3,7-bis(dimethylamino)phenothiazin-5-ium) is generated having $C\text{-}S^{+}\text{=}C$ bond functional group. Attack of $OH^{\bullet}$ on this functional group leads to the cleavage of bonds and (2a; 3-(3-(dimethylamino)cyclohexa-2,4-dien-1-yl)sulfinyl-N,N-dimethylbenzene-1,4diamine) is generated having m/z=303. The oxidation state of S now changes from -2 to 0 by the attack of $OH^{\bullet}$. This conversion to C-S(=O)-C ultimately leads to the opening of the central aromatic ring. Subsequent attack of $OH^{\bullet}$ finally leads to the formation of an intermediate (2b; phenol) with the release of NH_4^{+} and SO_4^{2-} ions. The intermediate (2b) then gets converted into benzoquinone (2c). This is further supposed to get mineralized into stable

View Article Online
DOI: 10.1039/C6RA17555D

CO_2.[57] Degradation of MB also results in the formation of 2*H*-1,4-thiazene (3) having m/z=98, which ultimately gets mineralized into CO_2, NO_3^-, NH_4^+ and SO_4^{2-} ions. Attack of active $OH^\bullet$ species can also take place at C-5 position, leading to the formation of intermediate (4; 3,4,5-trihydroxy-9,10-dioxo-dihydroanthracene-2-sulfonic acid), which gets converted into 6-formyl-3,4-dihydroxy-5,8-dioxo-5,8-dihydrophthalene-2-sulphonic acid (4a; m/z=295). This ultimately gets cleaved into but-2-enal (4b; m/z=71). In another proposed pathway for the degradation of MB, an intermediate (5; 3,7-bis(dimethylamino)-9-formyl-4a*H*-phenothiazine-1-carboxylic acid) having m/z=355 is generated, which after series of oxidative and bond cleavages results in the formation of (5a; (*Z*)- 2-aminoethenethiol; m/z=73). This species is also supposed to get mineralized into NO_3^-, NH_4^+ and SO_4^{2-} ions. In addition to this, various other by-products are also formed such as sulfur trioxide (6; m/z=83), 2,3-dimethyl cyclohexa-2,5-diene-1,4-dione (7; m/z=140) and benzoquinone (2c; m/z=108). Formation of CO_2, NO_3^-, NH_4^+ and SO_4^{2-} ions suggest complete mineralization of the dyes mixture.

4. Reusability of catalyst

To test the reusability of the catalystin simulated water treatment containing ARS and MB, the decolorization reaction was run with a 180 min cycle. At the end of each cycle, TMO nanoparticles were separated, heated to 60 ºC for 30 min, followed by washing with acetone as well as distilled water, and further used for next cycle. The results showed that TMO nanoparticles could be reused at least ten times (Figure 1S) without a significant loss in its adsorbing properties.

5. Environmental concern of hazardous dyes

View Article Online
DOI: 10.1039/C6RA17555D

Industries such as textiles, cosmetics, paper, printing, *etc*., involve the use of dyes in form of their aqueous solution and discharge them untreated into the water reservoirs. The amount of dyes discarded each year is constantly increasing which is the major reason for environmental pollution. Moreover, use of reactive dyes worldwide has increased from 60,000 tonnes in 1988 to 178,000 tonnes in 2004.[58] Clinical and immunological investigation revealed that about 15% of 400 workers exposed to reactive dyes experienced nasal and respiratory problems.[59] Exposure to such dyestuffs causes serious health hazards since these have a property of binding to the body proteins.[60] In early 1981 some sulphonyl ethyl sulphatederivates were observed to be carcinogenic[60] and various textile dyes and their raw materials including benzidine and o-toluidine based are included in the international register of cancer-causing chemicals.[61]

In order to regulate this negative impact of dyes on living species, several methods such as physical separation, chemical processes and biological degradation are being carried out. Due to the growing awareness worldwide researchers are showing keen interest in the development of effective removal techniques. Some important techniques are widely used including adsorption, oxidation, coagulation–flocculation, biological treatment, electrochemical treatment and membrane filtration. This needs further advancement so that it can be employed on a large scale.

6. Conclusions

A quick green approach using sunlight and water for synthesis ofZnO, CuO, Co_3O_4, NiO and Cr_2O_3 nanostructures was successfully established. Almost uniformly distributed TMO nanoparticles were obtained with distinct morphologies such as nanotubes (ZnO), nanorods (CuO), nanorods, triangles and hexagons (Co_3O_4), needle-shaped (NiO) and nanobeads (Cr_2O_3). These TMOs were found to be potential catalystin treatment of simulated water containing hazardous dyes: ARS + MB. Among all, the degradation efficiency of Cr_2O_3 was highest

View Article Online
DOI: 10.1039/C6RA17555D

(10mg/L of dye; 15 mg catalyst loading and neutral pH) followed by ZnO > CuO > NiO > Co_3O_4, depending on the size of respective TMO. The finding of small and non-toxic by-products like but-2-enal, sulfur trioxide and benzoquinone indicates the positive aspects of using synthesized nanoparticles in removal of toxic dyes. Some oxidativeby-products such as 2*H*-1,4-thiazene-2,3,6-triol, 2*H*-1,4-thiazene, 2,3-dimethylcyclohexa-2,5-diene-1,4-dione, maleic acid and malealdehyde were identified. Further spread of TMO nanoparticles utilization in waste water treatment for the removal of several other harmful pollutants such as polycyclic aromatic hydrocarbons (PAHs), aromatic amines, various types of phenols and other carcinogenic materialsneeds to be explored more effectively. In addition to this, the reusability of the catalyst can decrease the cost of process.

Acknowledgements

Authors are thankful to DST-FIST New Delhi for providing the equipment (UV-VIS spectrohpotometer) used in characterization of the samples. Authors are also thankful to NIPER Mohali for Zeta potential analysis and SAIF Panjab University, Chandigarh for TEM analysis. One of the authors Ms. Vidhisha Jassal is thankful to Ministry of Human Resource Development (MHRD), New Delhi for providing fellowship.

View Article Online
DOI: 10.1039/C6RA17555D

References

1. M.A. Laguna-Marco, D. Haskel, N. Souza-Neto, J.C. Lang, V.V. Krishnamurthy, S. Chikara, G. Cao and M. van Veenendaal, *Phys. Rev. Lett*., 2010, **105**, 216407.
2. B. J. Kim, H. Jin, S. J. Moon, J. Y. Kim, B. G. Park, C. S. Leem, J. Yu, T. W. Noh, C. Kim, S. J. Oh, J. H. Park, V. Durairaj, G. Cao and E. Rotenberg, *Phys. Rev. Lett*., 2008, **101**, 076402.
3. F. Jiao and H.Frei, *Energy Environ. Sci*., 2010, **3**, 1018.
4. W. Y. Li, L. N.Xu andJ. Chen, *Adv. Funct. Mater*., 2005, **15**, 851.
5. P. Poizot, S. Laruelle,S. Grugeon,L. Dupont and J. M. Tarascon, *Nature*, 2000, **407**, 496.
6. X. H. Lu, J. Lei, D. Zhou, S. Y. Fang, Y. L. Dong and Q. H. Xia, *Indian J. Chem. A: Inorg. Bio-Inorg. Phys. Theor. Anal. Chem*., 2010, **49**, 1586.
7. M. Te and H. C. Foley, *Appl. Catal. A*: *Gen.*, 1994, **119**, 97.
8. X. Y. Deng and Z. Chen, *Mater. Lett*., 2004, **58**, 276.
9. H. Mohebbi, T. Ebadzadeh and F. A. Hesari, *J. Power Sources*, 2008, **178**, 64.
10. J. A. Linthorst, *Found. Chem*., 2010, **12**,55.
11. P. T. Anastas and J. B. Zimmerman, Why we need a green nano award & how to make it happen. Washington DC: Woodrow Wilson International Center for Scholars,2007, 1.
12. J. E. Hutchison, *ACS Nano*., 2008, **2**, 395.
13. P. Raveendran,J. Fu and S. L. Wallen, *J. Am. Chem. Soc*., 2003, **125**, 13940.
14. S. H. S. Chan, T. Y. Wu, J. C. Juan and C. Y. The, *J. Chem. Technol. Biotechnol*., 2011, **86**, 1130.
15. T. Robinson, G. McMullan, R. Marchant and P. Nigam, *Bioresour. Technol*., 2004, **77**, 247.
16. V.Jassal, U. Shanker, B. S. Kaith, S. Shankar, *RSC Adv*., 2015, **5**, 26141.
17. S. Prillo,M. L. Ferreira and E. H. Rueda, *J. Hazard. Mater*., 2009, **168**, 168.

View Article Online
DOI: 10.1039/C6RA17555D

18. J. Kurepa, T. Paunesku, S. Vogt, H. Arora, B. M. Rabatic, J. Lu, M. B. Wanzer, G. E. Woloschak and J. A. Smalle, *Nano Lett*., 2010, **10**, 2296.

19. K. V. Kumar, V. Ramamurthi and S. Sivanesan, *J. Colloid Interf. Sci*.,2005, **284**, 14.

20. V. Vadivelan and K. V. Kumar, *J. Colloid Interf. Sci*., 2005, **286**, 90.

21. S. M. Shaban, I. Aiad, M. M. Sukkary, E. A. Soliman, and M. Y. Awady, *Chin. Chem. Lett*., 2015, **26**, 1415.

22. G. A. Bhaduri, R. Little, R. B. Khomane, S. U. Lokhande, B. D. Kulkarni, B. G. Mendis, and L. Siller, *J. Photochem. Photobiol. A Chem*., 2013, **258**, 1.

23. M. Guan, Z. Zhou, R. Duan, B. Du, X. Li, L. Liu and Q. Zhang, *RSC. Adv*., 2015, **5** 26540.

24. A. Nugroho and J. Kim, *J. Ind. Eng. Chem*., 2014, **20**, 4443.

25. M. Salavati-Niasari, A. Khansari and F. Davar, *Inorg. Chim. Acta*, 2009, **362**, 4937.

26. H. Yang, Y. Hu, X. Zhang andG. Qiu, *Mater. Lett*., 2004, **58**, 387.

27. J. Ahmed, T. Ahmad, K. V. Ramanujachary, S. E. Lofland and A. K. Ganguli, *J. Colloid Interface Sci*., 2008, **321**, 434.

28. M. Tadic, D. Nikolic, M. Panjan, and G. R. Blake, *J. Alloys. Compd*., 2015, **647,** 1061.

29. M. Salavati-Niasari, F. Davar and Z. Fereshteh, *J. Alloys Compd*., 2010, **494**, 410.

30. N. Dharmaraj, P. Prabu, S. Nagarajan, C. H. Kim, J. H. Park and H.Y. Kim, *Mat. Sci. Eng. B-Solid*, 2006, **128**, 111.

31. P. Gibot, and L. Vidal, *J. Eur. Ceram. Soc*., 2010, **30**, 911.

32. N. R. Jana , Y. Chen and X. Peng, *Chem. Mater.*, 2004, **16**, 3931.

33. V. Anand, and V. C. Srivastava, *J. Alloys. Compd*., 2015**, 636,** 288.

34. S. Hingorani, V. Pillai, P. Kumar, M. S. Multani and D. O. Shah, *Mater. Res. Bullet.*, 1993, **28**, 1303.

35. L. Wang and M. Muhammed, *J. Mater. Chem.*, 1999, **9**, 2871.

View Article Online
DOI: 10.1039/C6RA17555D

36. A. Becheri, M. Dürr, P. L. Nostro and P. Baglioni, *J. Nanopart. Res*., 2008, **10**, 679.

37. K. Phiwdanga, S. Suphankija, W. Mekprasarta, and W. Pecharapa, *Energy. Procedia*., 2013, **34**, 740.

38. M. Salavati-Niasari and F. Davar, *Mater. Lett*., 2009, **63**, 441.

39. H. Q. Wu, X. W. Wei, M. W. Shao, J. S. Gu and M. Z. Qu, *Chem. Phys. Lett*., 2002, **364**, 152.

40. C. B. Ong, A. W. Mohammad,R. Rohani,M. M. Ba-Abbad and N.H.H. Hairom, *Process. Saf. Environ. Prot*., 2016, http://dx.doi.org/10.1016/j.psep.2016.04.006.

41. N. H. H. Hairom, A. W. Mohammad and A. A. H. Kadhum, *Sep. Purif. Technol*., 2014, **137**, 74.

42. K. Jeyasubramanian, G. S. Hikku and R. K. Sharma, *J. Water Proc. Eng*., 2015, **8**, 35.

43. S. K. Kansal, R. Lamba, S. K. Mehta and A. Umar, *Mat. Lett*., 2013, **106**, 385–389.

44. M. U. A. Prathap, B. Kaur and R. Srivastava,*J. Colloid Interface Sci.*, 2012, **370**, 144.

45. M. Vaseem, A. Umar, Y.B. Hahn, D.H. Kim,K.S. Lee, J.S. Jang, J.S. Lee, *Catal. Commun*., 2008, **10**, 11.

46. A. D. Bokare, R. C. Chikate, C. V. Rode and K. M. Paknikar, *Appl. Catal. B*: *Environ*., 2008, **79**, 270.

47. N. Daneshvar, D. Salari and A. R. Khataee, *J. Photochem. Photobiol*., 2004, **162**, 317.

48. X. Zhang, Y. Wang and G. Li, *J. Mol. Catal. A Chem*., 2005, **237**, 199.

49. M. A. Tariq, M. Faisal and M. Muneer, *J. Hazard. Mater*., 2005, **127**,172.

50. L. Mu, S.S. Feng, *J. Control. Release*, 2001, **76**. 239.

51. R. Sankar, A. Karthik, A. Prabu, S. Karthik, K.S. Shivashangari and V. Ravikumar, *Colloids Surf. B*, 2013, **108**, 80.

52. L. Lin, P. Qiu, X. Cao and L. Jin, *Electrochim. Acta*, 2008,**53**, 5368.

53. M. B. Kasiri and H. Aleboyeh, *Appl. Catal. B: Environ*., 2008, **84**, 9.

View Article Online
DOI: 10.1039/C6RA17555D

54. V. Jassal, U. Shanker and B. S. Kaith, *Scientifica*, 2016, **2016**, 1.

55. Viladkar, T. Alam and Kamaluddin, *J. Inorg. Biochem*., 1994, **53**, 69.

56. G. Liu, X. Li, J. Zhao, S. Horikoshi, H. Hidaka, *J. Mol. Catal. A: Chem*., 2000, **153**, 221.

57. A. Houas, H. Lachheb, M. Ksibi, E. Elaloui, C. Guillard, J. M. Herrmann, *Appl. Catal. B*: *Environ*., 2001, **31**, 145.

58. D. Phillips, *J. Soc. Dyers Colour*., 1996, **112**, 183.

59. A. Docker, J. M. Wattie, M. D. Topping, C. M. Luczynska, A. J. N. Taylor, C. A. C. Pickering, P. Thomas and D. Gompertz,*Br. J. Ind. Med*.,1987, **44**, 534.

60. T. Keneklis, Fiber reactive dye toxicological profiles, U.S. Consumer Product Safety Commission, Washington D.C., Contact No.CPSC-C-81-1110, 1981, 271.

61. IARC. Benzidine- based dyes. IARC Monographs on evaluation of carcinogenic risk to humans, IARC, Lyon 1987, **29**.

View Article Online
DOI: 10.1039/C6RA17555D

Abstract Graphic

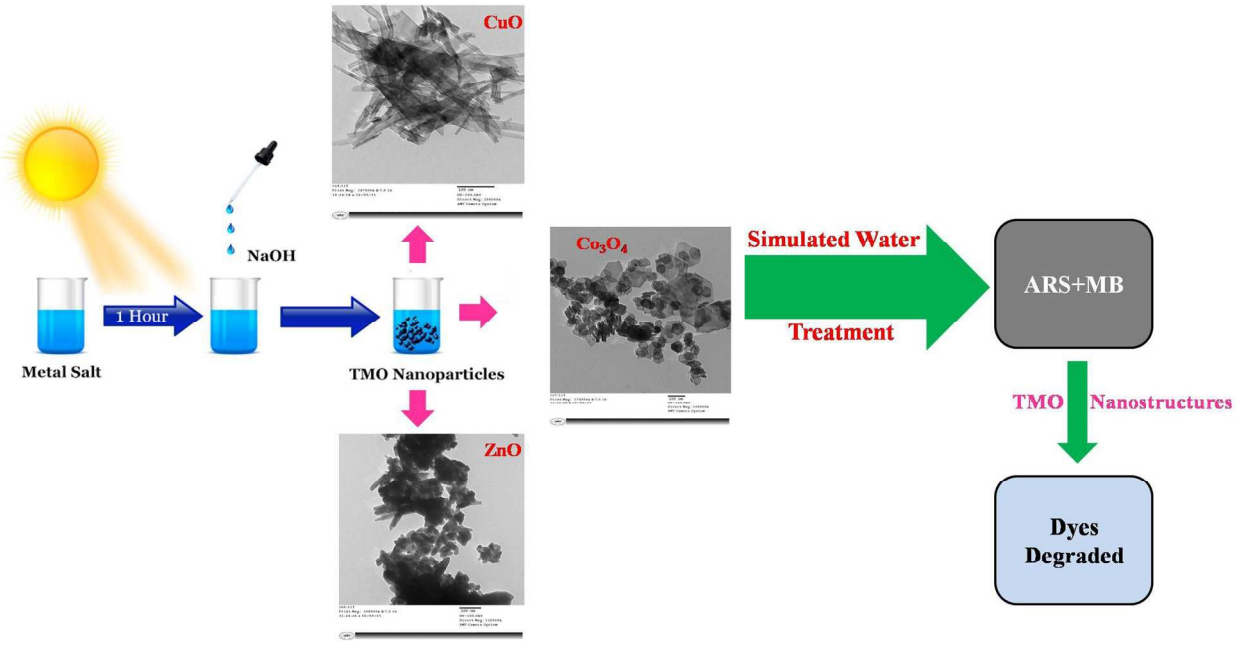

Synopsis: Novelty of work lies in utilizing sunlight irradiated green synthesis of TMO nanoparticles and potential in simulated water treatment.

List of Figures

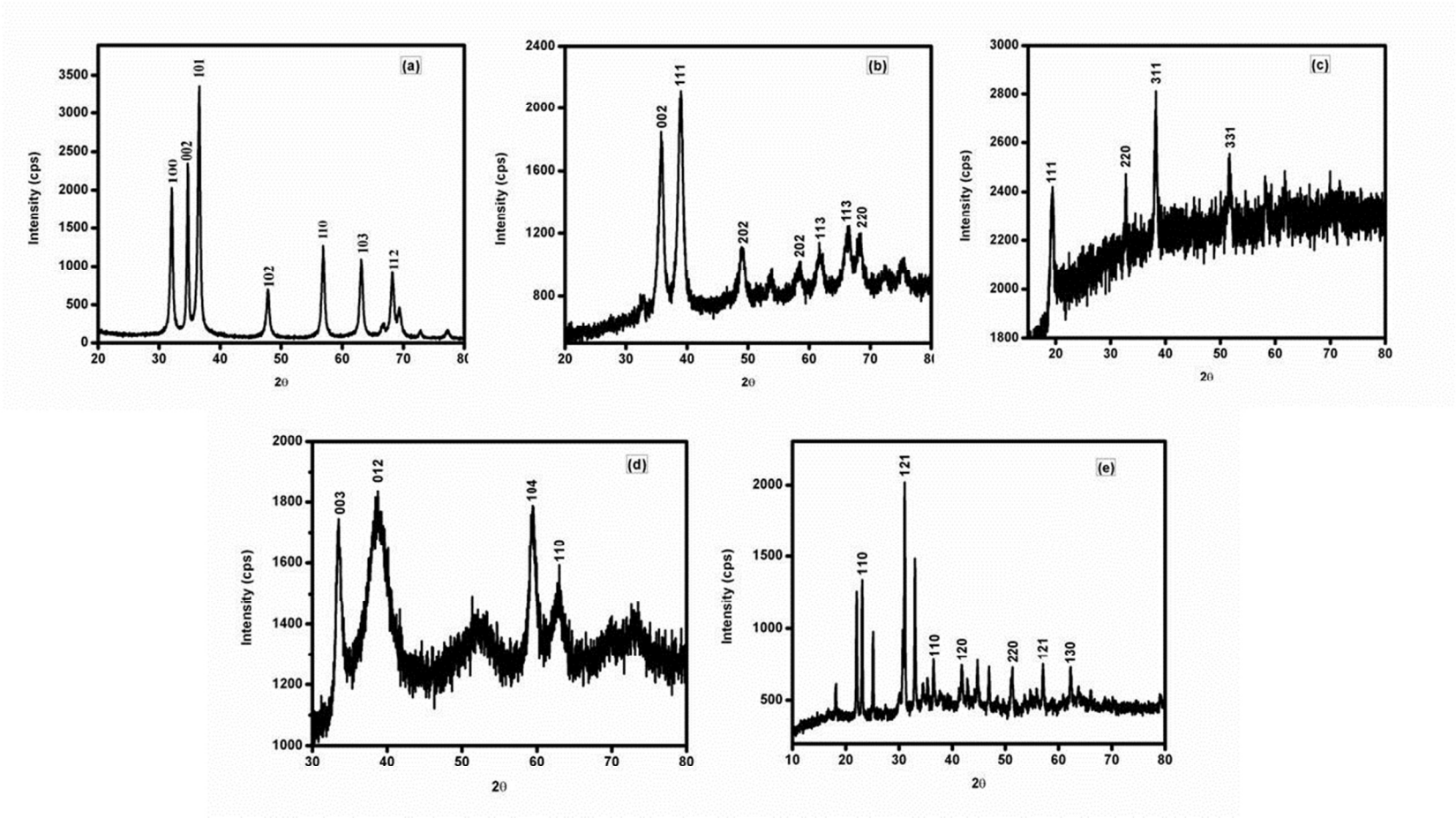

Figure 1. PXRD pattern of (a) ZnO (b) CuO (c) Co_3O_4 (d) NiO (e) Cr_2O_3 nanoparticles

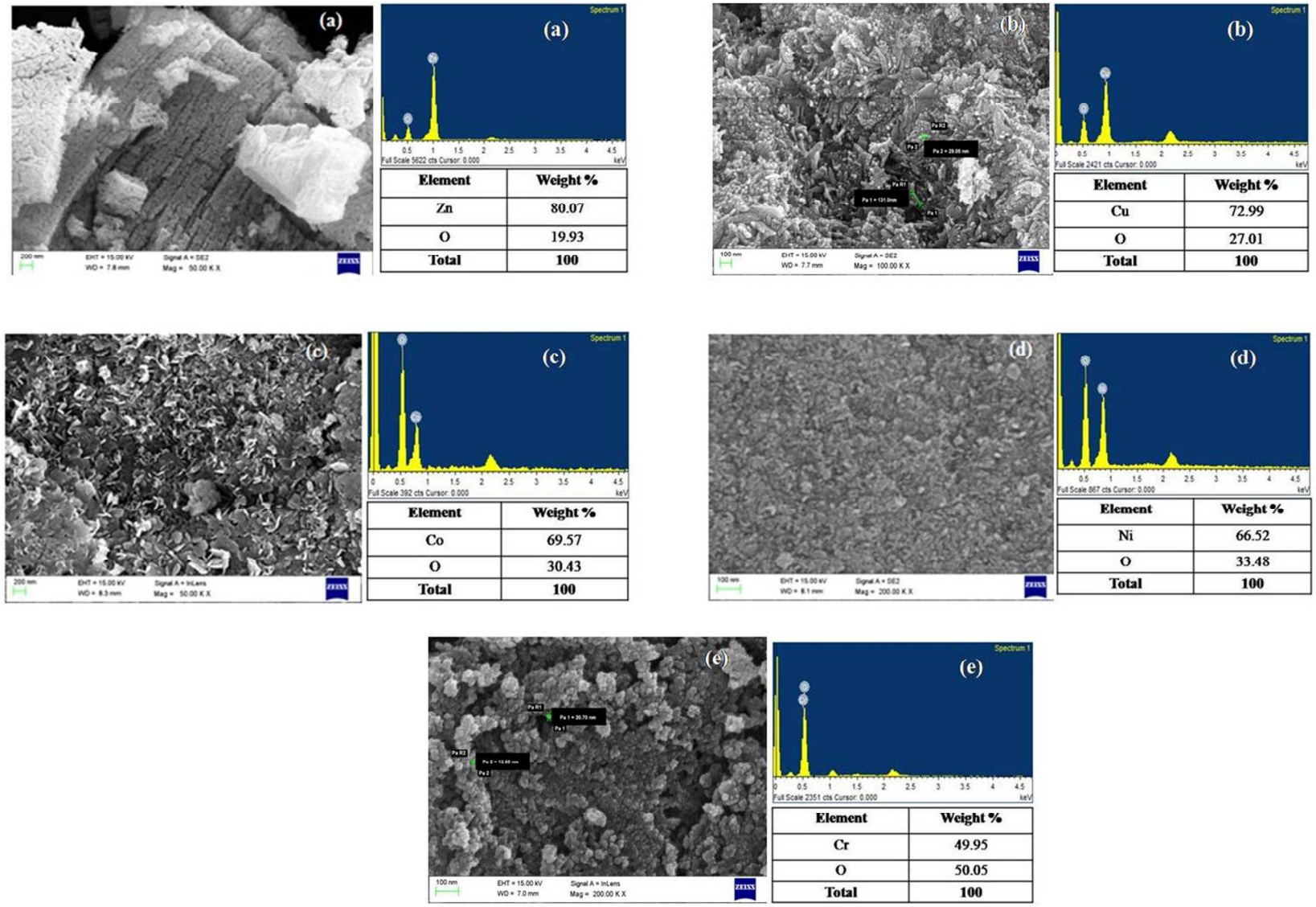

Figure 2. FE-SEM and EDS analysis of (a) ZnO (b) CuO (c) Co_3O_4 (d) NiO (e) Cr_2O_3 nanoparticles

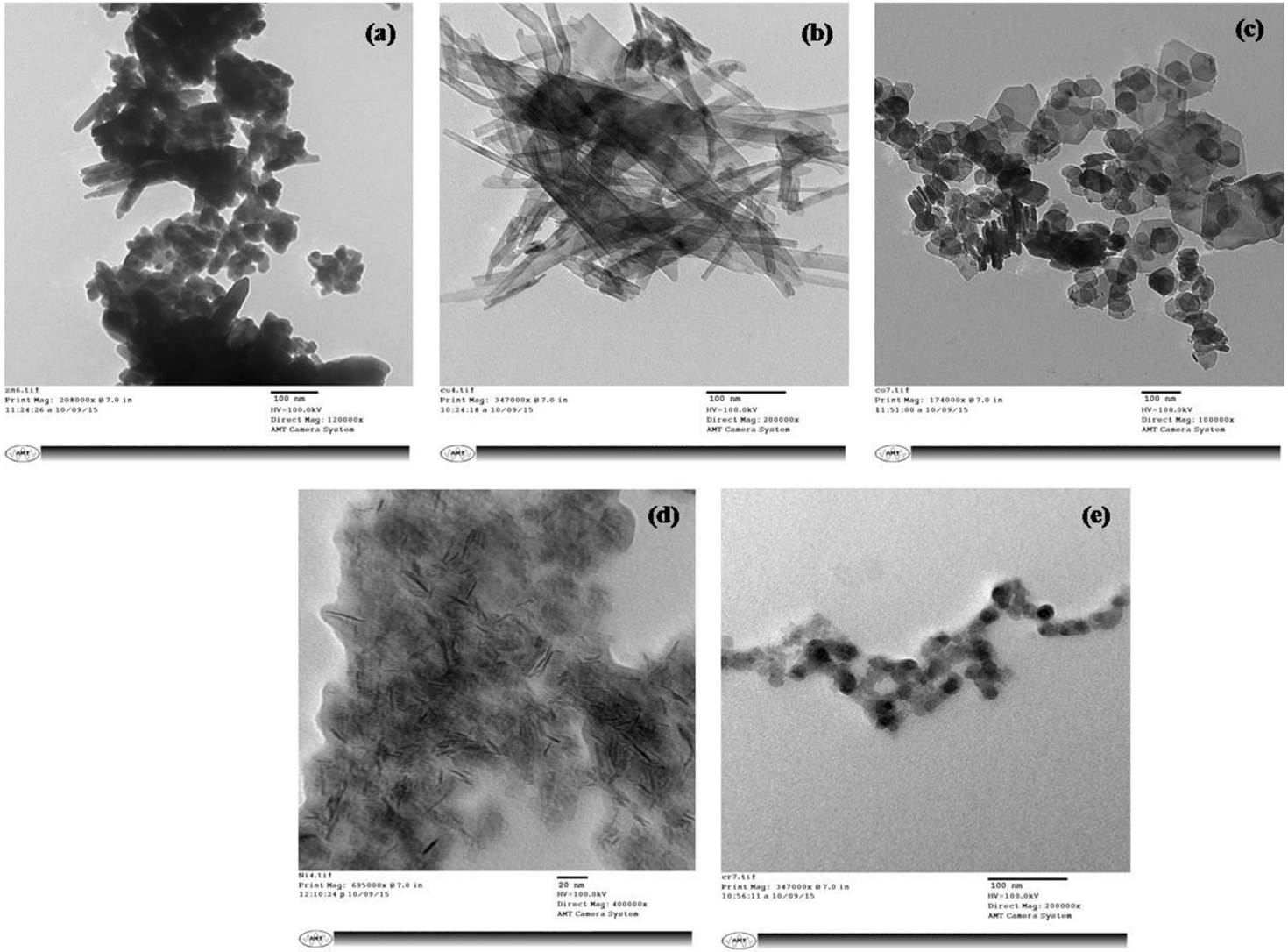

Figure 3. TEM images of (a) ZnO (b) CuO (c) Co_3O_4 (d) NiO (e) Cr_2O_3 nanoparticles

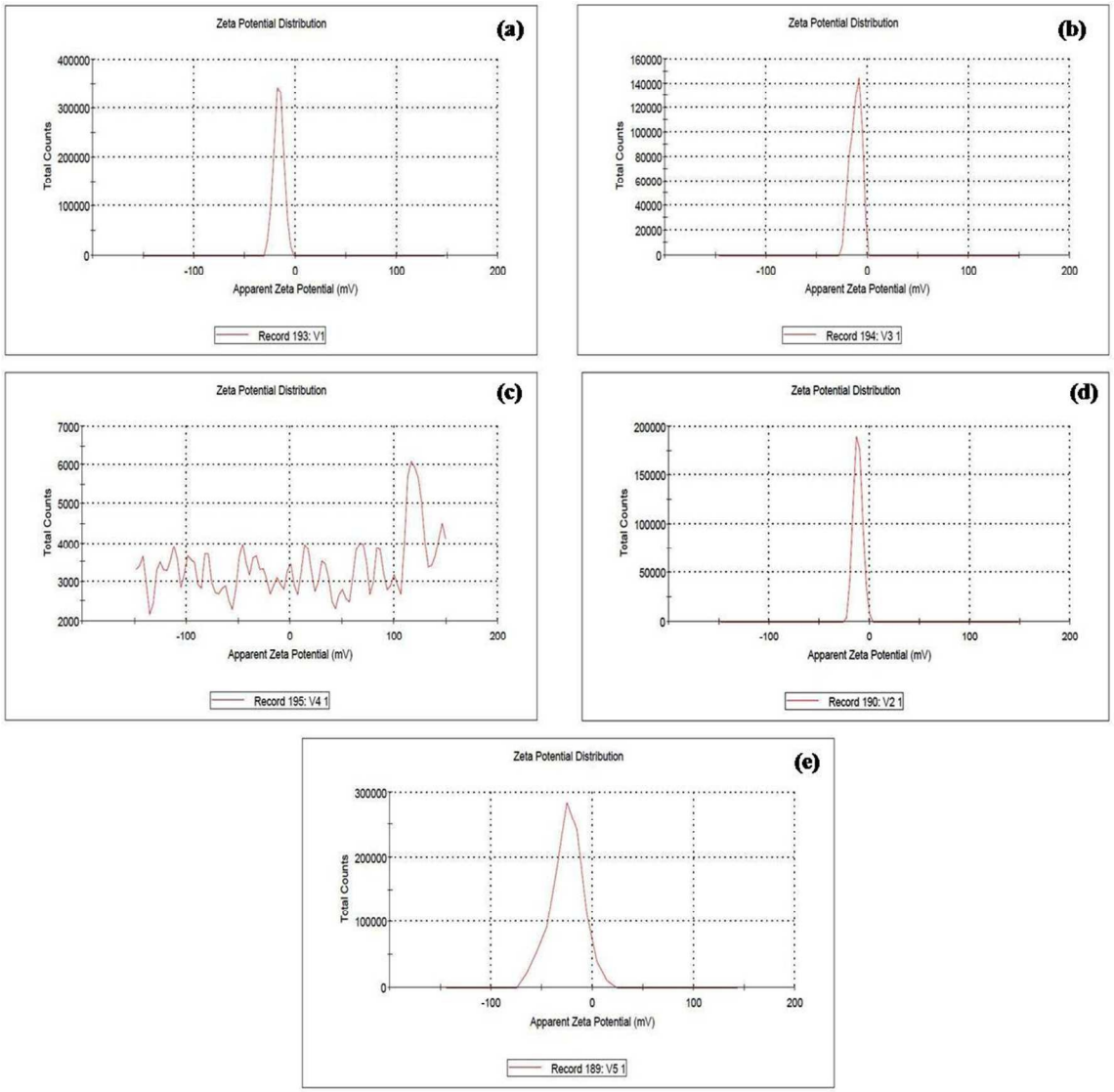

Figure 4. Zeta potential measurement of (a) ZnO (b) CuO (c) Co_3O_4 (d) NiO (e) Cr_2O_3 nanoparticles

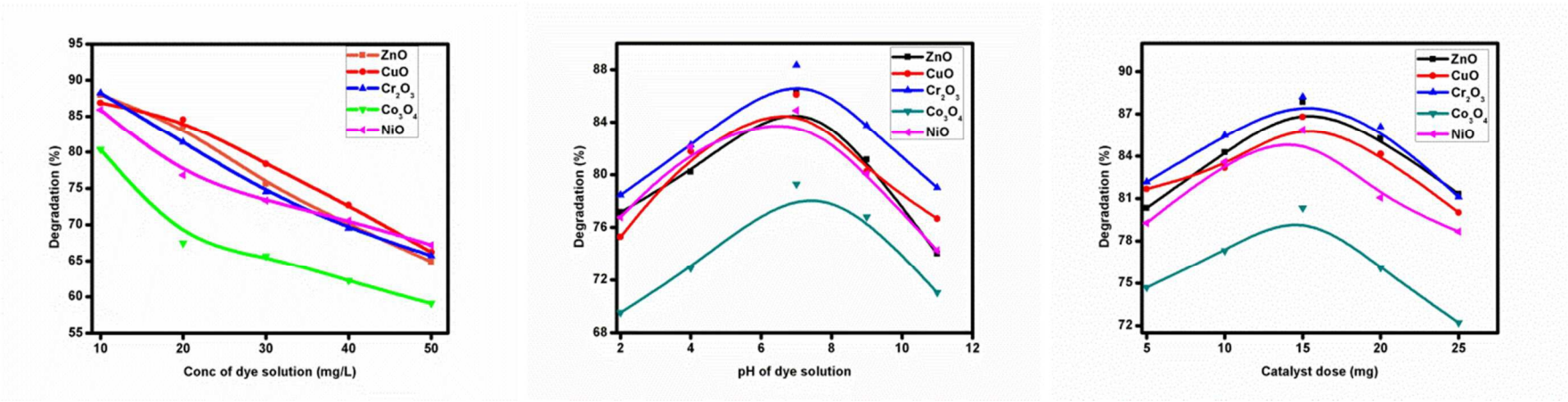

(a) (b) (c)

Figure 5. Dye degradation (%) at different (a) dye concentrations (b) pH (c) catalyst dose

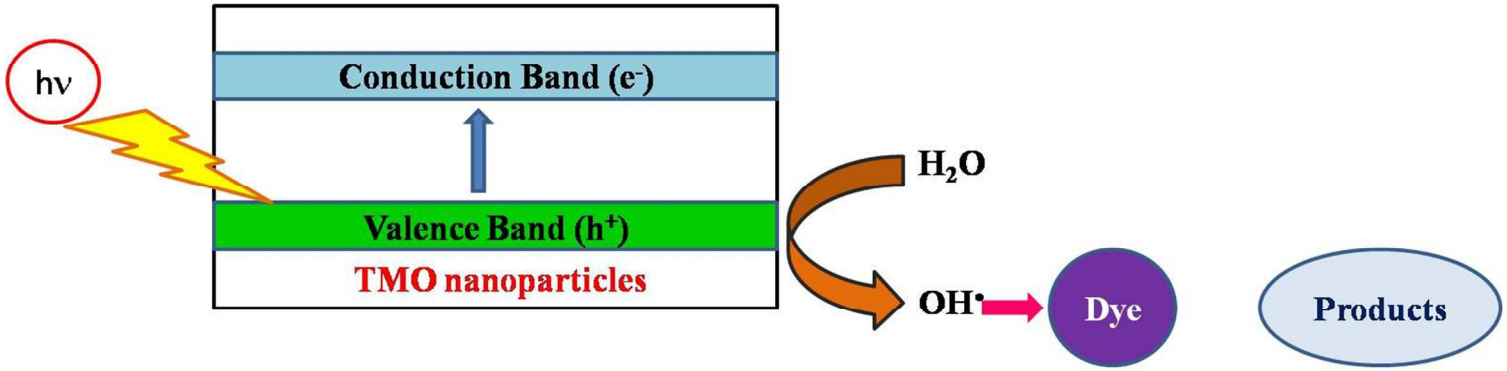

Figure 6. Schematic diagram of photocatalytic dye degradation

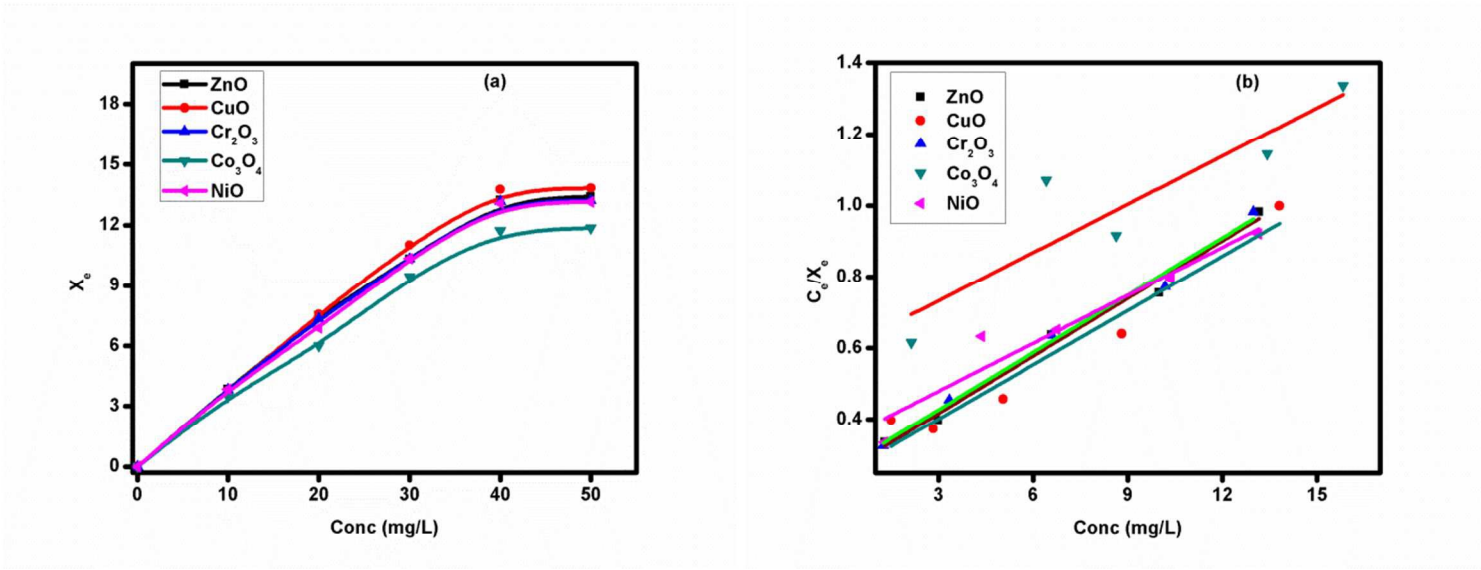

Figure 7. (a) Adsorption isotherm; (b) Langmuir isotherms for adsorption of Alizarin Red S (ARS) +Methylene Blue (MB) on different transition metal oxide (TMO) nanoparticles

View Article Online
DOI: 10.1039/C6RA17555D

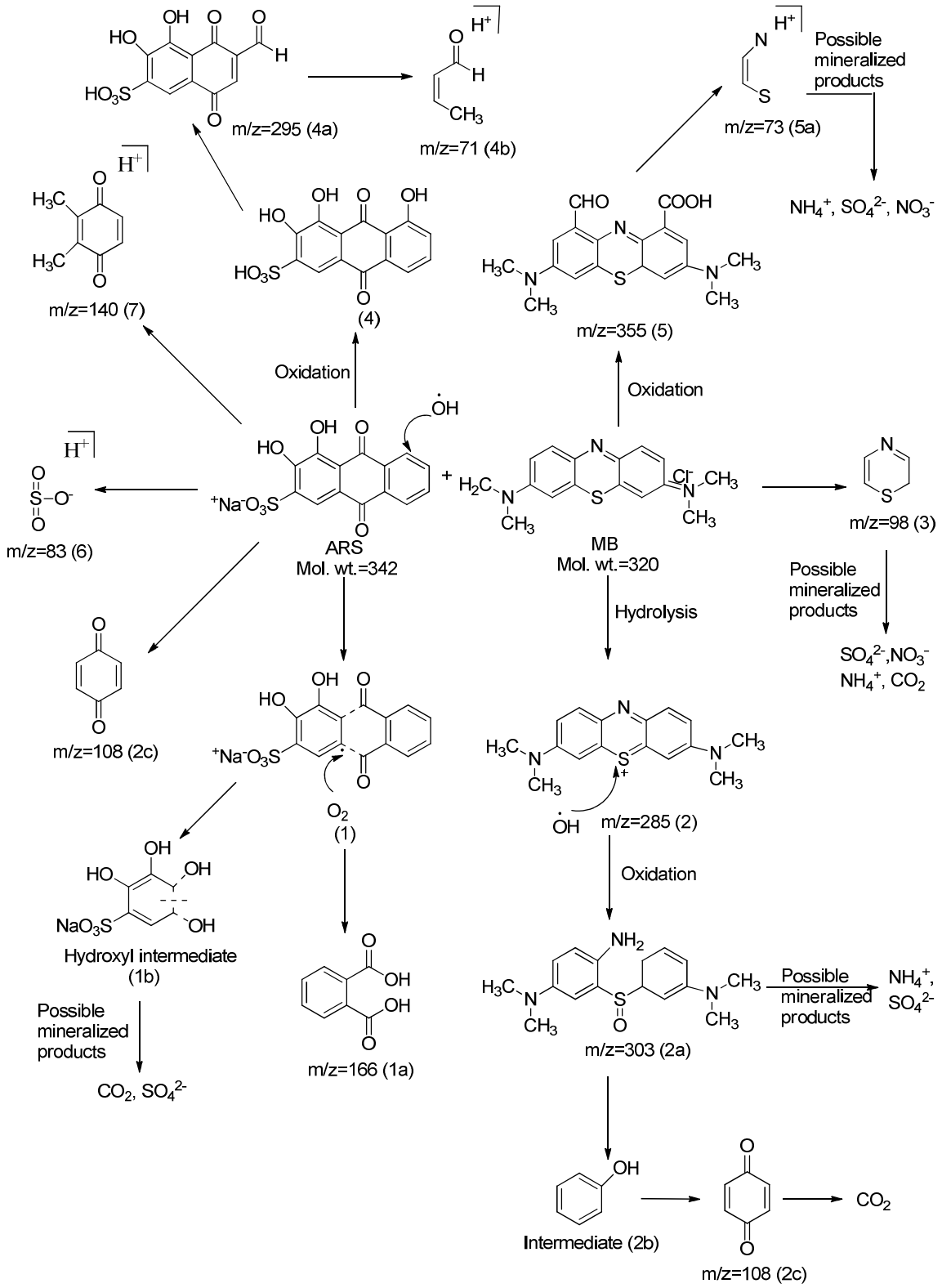

Figure 8. Proposed Degradation pathway of ARS and MB using TMO nanostructures

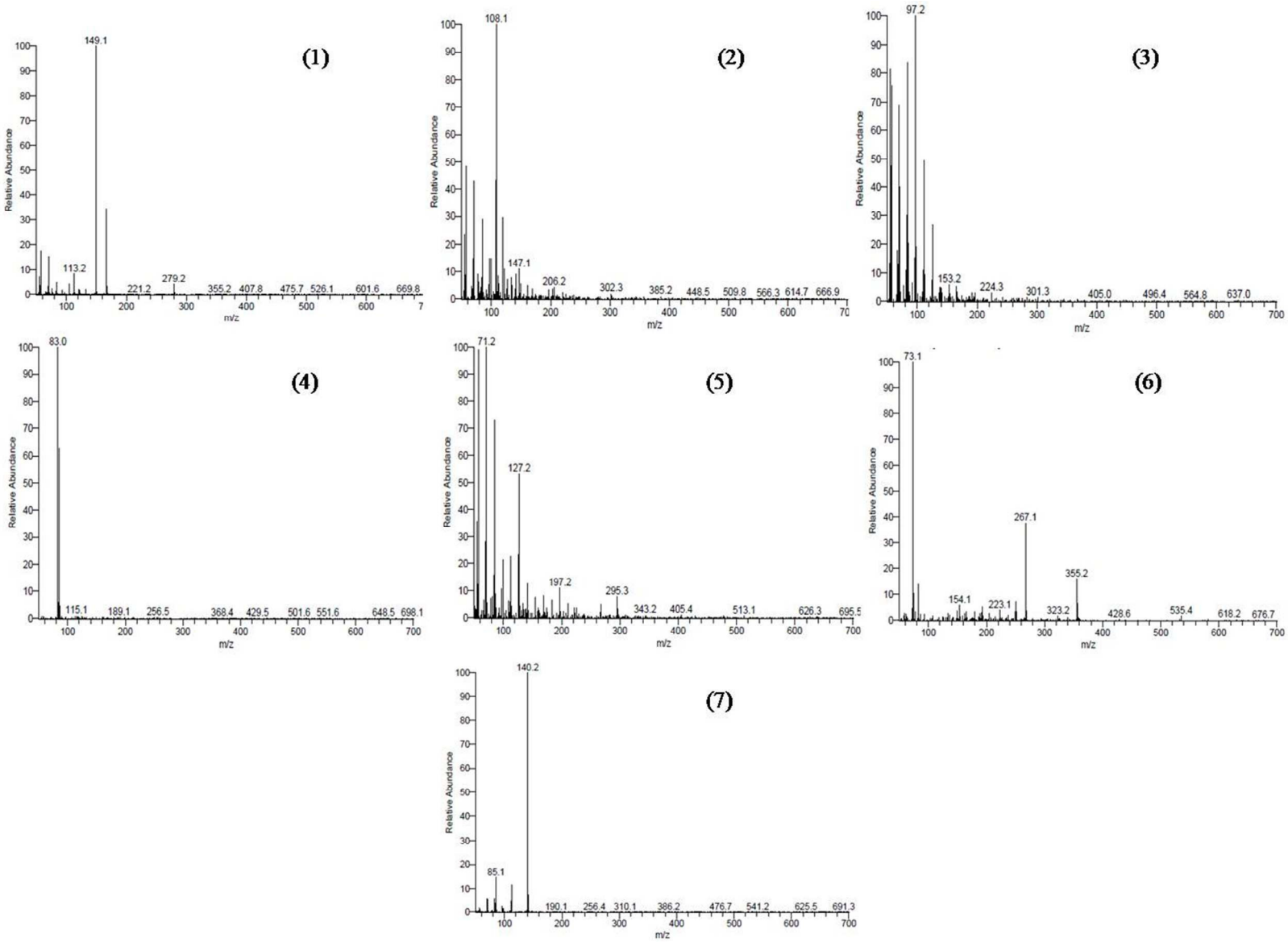

Figure 9. Representative mass spectra of various degraded products formed

View Article Online
DOI: 10.1039/C6RA17555D

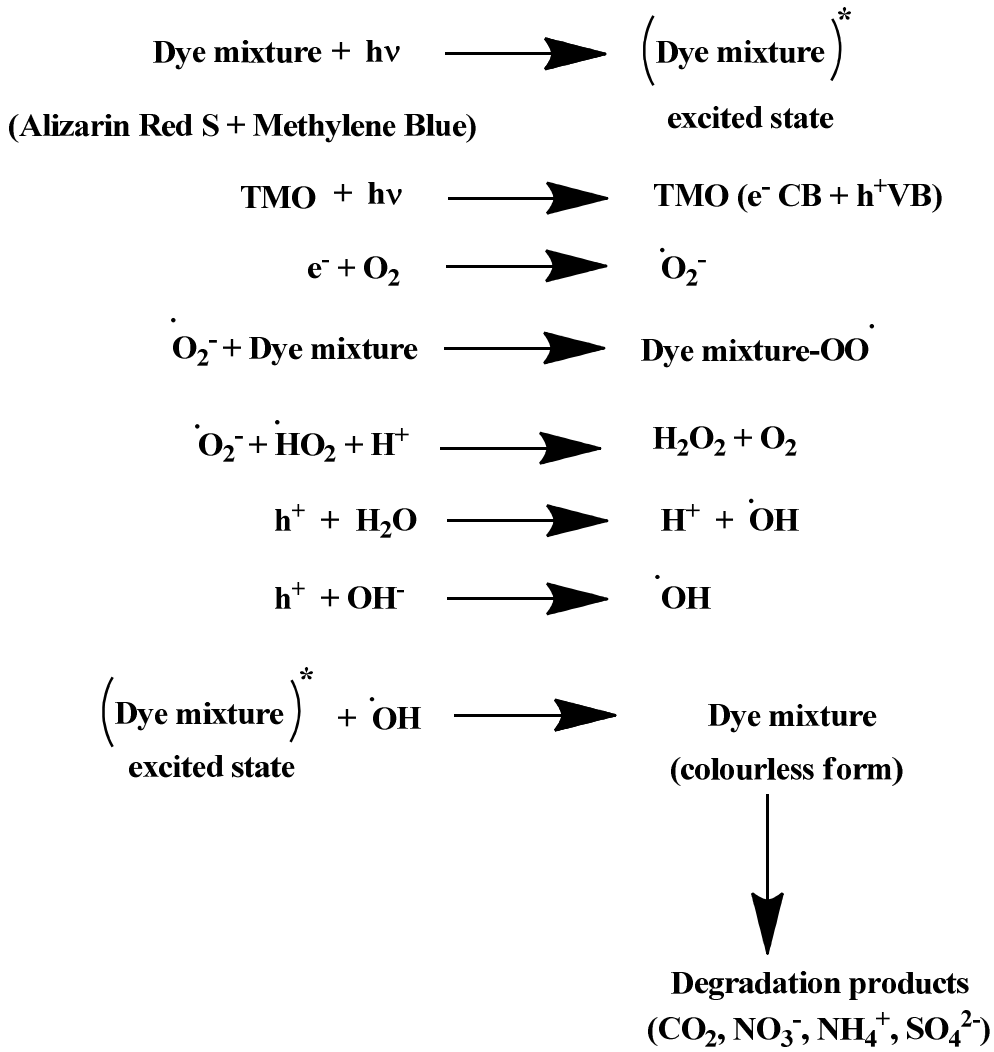

Figure 10. Photocatalytic degradation of ARS and MB in presence of TMO nanoparticles